



# CHORUS

This is the accepted manuscript made available via CHORUS. The article has been published as:

## Origin of p-type conductivity in layered $n\text{GeTe}\cdot m\text{Sb}_2\text{Te}_3$ chalcogenide semiconductors

Zhimei Sun, Yuanchun Pan, Jian Zhou, Baisheng Sa, and Rajeev Ahuja

Phys. Rev. B **83**, 113201 — Published 22 March 2011

DOI: [10.1103/PhysRevB.83.113201](https://doi.org/10.1103/PhysRevB.83.113201)

# Origin of $p$ -type conductivity in layered $n\text{GeTe}\cdot m\text{Sb}_2\text{Te}_3$ chalcogenide semiconductors

Zhimei Sun,<sup>1,2\*</sup> Yuanchun Pan,<sup>1</sup> Jian Zhou,<sup>1</sup> Baisheng Sa,<sup>1</sup> Rajeev Ahuja<sup>3</sup>

<sup>1</sup>*Department of Materials Science and Engineering, College of Materials, Xiamen University, 361005 Xiamen, China*

<sup>2</sup>*Fujian Provincial Key Laboratory of Theoretical and Computational Chemistry (Xiamen University), China*

<sup>3</sup>*Department of Physics and Astronomy, Uppsala University, Box 520, 75120 Uppsala, Sweden*

$\text{Ge}_2\text{Sb}_2\text{Te}_5$ , an extensively studied narrow band gap semiconductors for phase-change memories, always displays  $p$ -type conductivity. However, the defect physics and origin of the  $p$ -type conductivity are not yet clear. We have studied various types of defects in layered  $n\text{GeTe}\cdot m\text{Sb}_2\text{Te}_3$  (GST) using *ab initio* calculations. The results show that the formation energies of  $V_{\text{Ge}}$  are always the lowest followed by  $\text{Sb}_{\text{Te}}$  in the studied GST. The majority defects are  $V_{\text{Ge}}$  and  $\text{Sb}_{\text{Te}}$ , which results in the  $p$ -type conductivity of GST. Although  $\text{Ge}_2\text{Sb}_2\text{Te}_5$  always has  $p$ -type character, one can make both  $p$  and  $n$  type  $\text{GeSb}_2\text{Te}_4$  and  $\text{GeSb}_4\text{Te}_7$  by tuning the atomic chemical environments.

PACS numbers: 61.72.J-, 61.72.jd, 71.20.Nr, 71.15.Nc

\* To whom correspondence should be addressed.  
Email: zmsun@xmu.edu.cn; zhmsun2@yahoo.com  
Tel: +86-592-2182617, Fax: +86-592-2186664

Point defects, such as vacancies, antisite and interstitial atoms, play an important role in the electrical properties of semiconductors. For example, the native defects of  $Zn_i$  and  $V_O$  in ZnO are the origin of its  $n$ -type conductivity and the difficulty of making it  $p$ -type for this technologically important semiconductor.<sup>1</sup> In contrast to ZnO, all the reported work on layered  $nGeTe \cdot mSb_2Te_3$  (GST) reveals  $p$ -type conductivity.<sup>2-4</sup> These chalcogenide semiconductors, such as  $Ge_2Sb_2Te_5$  ( $n=2, m=1$ ) and  $GeSb_2Te_4$  ( $n=1, m=1$ ), are technologically important recording materials for optical data storage and nonvolatile electronic memories or phase-change random access memories.<sup>5,6</sup> Even though experimental measurements have shown  $p$ -type conductivity in the amorphous, rock-salt and hexagonal or trigonal states of GST chalcogenides,<sup>6</sup> the defect physics and origin of  $p$ -type conductivity have been neglected for quite a long time whereas a significant attention has been focused on the structure and reversible phase-change mechanism in the phase-change community.<sup>5,6</sup> However, understanding of the defects and  $p$ -type conductivity in GST is important for tuning the performance in the memories. On the other hand, stable GST chalcogenides that crystallize in a hexagonal or trigonal structure have been investigated to be promising candidate materials even for thermoelectric applications.<sup>2</sup> For thermoelectric applications, it is important to unravel the origin of  $p$ -type conductivity and defect physics in order to make both  $p$  and  $n$  type conductivity be achieved in the same material. By the above motivations, in this work, we have performed extensive *ab initio* calculations and made an analysis to unravel the defect physics and origin of  $p$ -type conductivity in GST semiconductors.

As far as we know, the origin of  $p$ -type conductivity in amorphous chalcogenides was

attributed to the role of lone-pair electrons and charged defects based on the analysis of a valence-alternation-pairs model by Kolobov.<sup>7</sup> For crystalline GST, Ge or Sb vacancies have been suggested as the main reason of *p*-type conductivity in hexagonal GST225.<sup>6</sup> It is known that  $V_{\text{Ge}}$  and  $\text{Sb}_{\text{Te}}$  are the most readily formed defects in GeTe and  $\text{Sb}_2\text{Te}_3$ ,<sup>8,9</sup> respectively. Therefore, it is natural to apply the defect physics in GeTe and  $\text{Sb}_2\text{Te}_3$  to the GST pseudobinaries. We may also immediately suggest that the majority defect in GST will be  $V_{\text{Ge}}$  as  $n > m$  (e.g.  $\text{Ge}_2\text{Sb}_2\text{Te}_5$ ) and will be  $\text{Sb}_{\text{Te}}$  as  $n < m$  (e.g.  $\text{GeSb}_4\text{Te}_7$ ,  $n=1$ ,  $m=2$ ). In other words, the concentration of  $V_{\text{Ge}}$  decreases and that of  $\text{Sb}_{\text{Te}}$  increases as the ratio of  $n / m$  decreases. However, the above assumption is not completely true based on our present results. Below we will provide a fundamental understanding on the defects and origin of *p*-type conductivity in layered GST semiconductors.

Our *ab initio* calculations were performed based on the density functional theory as implemented in the VASP code.<sup>10</sup> We used projector-augmented-wave pseudopotentials (PAW) within the generalized gradient approximation (GGA) adopting the Perdew-Burke-Ernzerhof (PBE) exchange correlations.<sup>11,12</sup> An energy cutoff of 218.73 eV and Monkhorst-Pack grids of  $2 \times 2 \times 1$  for *k*-points sampling were used. We used  $\text{Ge}_2\text{Sb}_2\text{Te}_5$  (GST225),  $\text{GeSb}_4\text{Te}_7$  (GST147) and  $\text{GeSb}_2\text{Te}_4$  (GST124) to study the point defects in GST, where the former two compounds have a space group of  $P \bar{3}m1$  and GST124 has a  $R \bar{3}m$  symmetry.<sup>13</sup> We choose the lowest energy configurations which has building stackings of /Te/Ge/Te/Sb/Te/Te/Sb/ for the three compounds.<sup>14,15</sup> Supercells containing 81-, 84-, and 108-atoms were used for GST225, GST124 and GST147, respectively. The crystal structures were fully optimized in terms of volume and internal

atomic coordinates.

The formation energy of a neutral defect is calculated as follows:<sup>16</sup>

$$\Delta H_f = \Delta E(d) + n_{Ge}\mu_{Ge} + n_{Sb}\mu_{Sb} + n_{Te}\mu_{Te} \quad (1)$$

where

$$\Delta E(d) = E(d) - E(stoi.) + n_{Ge}\mu_{Ge}^{solid} + n_{Sb}\mu_{Sb}^{solid} + n_{Te}\mu_{Te}^{solid} \quad (2)$$

$E(d)$  and  $E(stoi.)$  are the total energies of the GST supercells with and without the defect, respectively.  $\mu_{Ge}^{solid}$ ,  $\mu_{Sb}^{solid}$  and  $\mu_{Te}^{solid}$  are the total energies of ground solid states Ge (diamond cubic), Sb (trigonal) and Te (trigonal), respectively.  $n_i$  are the number of atoms transferred from the supercell to the reservoir in order to create defects.  $\mu_{Ge}$ ,  $\mu_{Sb}$  and  $\mu_{Te}$  represent the atomic chemical potential of germanium, antimony and tellurium corresponding to the energy variation of an atom to or from a chemical reservoir, which is not necessary in solid ground states. To maintain the accuracy by error cancellation,  $E(d)$  and  $E(stoi.)$  are calculated with the same  $k$  points, cutoff energy, and supercell size.

Table I lists the formation energy of isolated neutral point defects for layered GST compounds. Herein  $Sb_{Te1}$  represents the Sb anti-atom being in the Te layer that locates between Te and Sb layers, while  $Sb_{Te2}$  represents the Sb anti-atom being in the Te layer that locates between Ge and Sb layers. For  $V_{Te1}$ , the missing Te atom locates between Ge and Sb layers, while that locates between Sb and Te layers for  $V_{Te2}$ . Some interesting conclusions can be obtained from Table I: (1) The formation energy of one  $V_{Ge}$  is always lower than that of one  $Sb_{Te}$  and the formation energy generally follows the sequence of  $Te_{Sb} > Sb_{Te2} > Sb_{Te1} > V_{Ge}$ , suggesting that neutral germanium vacancies are more likely to form than antisite atoms in layered GST; (2) All the calculated formation energies for

various types of defects in GST225 are the lowest among the three investigated compounds; (3) Antisite atom  $\text{Sb}_{\text{Te}}$  is more likely to form in the Te layers where weak Te-Te bond exists; (4) Forming one  $\text{V}_{\text{Sb}}$  is much easier in GST225 and the formation of  $\text{V}_{\text{Sb}}$  is unlikely in GST124 and GST147. We have also calculated the formation energy for defect pairs, for example, the formation energies of  $\text{V}_{\text{Ge}}+\text{Sb}_{\text{Te1}}$  are 0.810 and 0.811 eV in GST225 for the cases of the two defects being close and far, respectively. The calculated value are very close to that of  $H_f(\text{V}_{\text{Ge}}) + H_f(\text{Sb}_{\text{Te1}})$  that is 0.852 eV.

Based on the defect formation energies in Table I, the equilibrium defect concentrations were estimated by the formalism as follows:<sup>17</sup>

$$[D] = N_{\text{sites}} \exp\left(-\frac{H_f}{K_B T}\right) \quad (3)$$

Where  $[D]$  is the defect concentration,  $N_{\text{sites}}$  is the number of sites per unit volume of GST where point defects may be present,  $H_f$  is the formation energy,  $K_B$  and  $T$  are Boltzmann constant and temperature.

Fig. 1 (a) to (c) show the concentration of some selected point defects which are more likely to form in GST. It is interesting to note that in the three compounds, the  $\text{V}_{\text{Ge}}$  concentration is always the highest, followed by that of  $\text{Sb}_{\text{Te1}}$ , suggesting that the majority charge carrier in GST are holes, consequently result in the observed *p*-type conductivity. The defect concentrations of  $\text{Te}_{\text{Sb}}$  and  $\text{Sb}_{\text{Te2}}$  are several orders lower than that of  $\text{V}_{\text{Ge}}$  and  $\text{Sb}_{\text{Te1}}$ . The values of defect concentration at various temperatures can be read from Fig. 1. For example, if materials were synthesized at 1000 K which is slightly above the melting temperature, the  $\text{V}_{\text{Ge}}$  concentrations in GST225, GST124 and GST147 would be  $1.23 \times 10^{20} \text{ cm}^{-3}$ ,  $5.44 \times 10^{18} \text{ cm}^{-3}$  and  $3.63 \times 10^{18} \text{ cm}^{-3}$ , respectively, while the  $\text{Sb}_{\text{Te1}}$  concentrations

would be  $3.65 \times 10^{19} \text{ cm}^{-3}$ ,  $4.72 \times 10^{18} \text{ cm}^{-3}$  and  $4.00 \times 10^{18} \text{ cm}^{-3}$ , respectively. The calculated hole concentration in GST225 is in good agreement with that of the reported value of  $\sim 3 \times 10^{20} \text{ cm}^{-3}$ .<sup>6</sup> It is also interesting to note that the concentration of  $V_{\text{Ge}}$  and  $\text{Sb}_{\text{Te}}$  in GST225 are several orders higher than that in GST124 and GST147, with the latter two compounds have similar defect concentrations.

Further analysis shows that atomic chemical potentials drastically affect the defect formation energies in GST. As we know, among the three elements in GST, tellurium has the highest volatility and Ge is nonvolatile material. Therefore, experimentally it is most likely to have a Te deficient chemical environment and followed by a Sb deficient environment if we start from the nominal compositions to synthesize GST. A literature survey reveals that most of the experimental works only showed the nominal composition, however, a stoichiometric compound was hardly obtained as shown by the composition analysis. For example, in the work by Lyeo et al.,<sup>18</sup> the composition for GST225 is Ge:Sb:Te=22.5:23.3:54.2 that may be rewritten as Ge:Sb:Te(+Sb<sub>Te</sub>)=22.5:22.5:55, suggesting the existence of Sb<sub>Te</sub>. In contrast, another recent work showed a composition of Ge:Sb:Te=2.02:1.88:5.13 that may be rewritten as Ge:Sb(Te<sub>Sb</sub>):Te=2.02:2.01:5.00,<sup>19</sup> which suggests the existence of Te<sub>Sb</sub>. Therefore, in the present work, we considered the Sb or Te deficient condition. The defect formation energies with various atomic chemical potentials are estimated by the following restrictions for  $\{\mu_{\text{Ge}}, \mu_{\text{Sb}}, \mu_{\text{Te}}\}$ :

$$n_{\text{Ge}}\mu_{\text{Ge}} + n_{\text{Sb}}\mu_{\text{Sb}} + n_{\text{Te}}\mu_{\text{Te}} = \Delta H_f(\text{Ge}_{n_{\text{Ge}}}\text{Sb}_{n_{\text{Sb}}}\text{Te}_{n_{\text{Te}}}) \quad (1)$$

is required to maintain a stable  $n\text{GeTe} \cdot m\text{Sb}_2\text{Te}_3$ ;

$$\mu_{\text{Ge}} + \mu_{\text{Te}} \leq \Delta H_f(\text{GeTe}) \quad , \quad 2\mu_{\text{Sb}} + 3\mu_{\text{Te}} \leq \Delta H_f(\text{Sb}_2\text{Te}_3) \quad (2)$$

is required to prevent the formation of binaries.  $\mu_{Ge} \leq 0$ ,  $\mu_{Sb} \leq 0$ ,  $\mu_{Te} \leq 0$  are also needed to prevent the precipitation of solid elemental Ge, Sb and Te. Where our calculated  $\Delta H_f(\text{Ge}_2\text{Sb}_2\text{Te}_5) = -1.881\text{eV}$ ,  $\Delta H_f(\text{GeSb}_2\text{Te}_4) = -1.564\text{eV}$ ,  $\Delta H_f(\text{GeSb}_4\text{Te}_7) = -2.464\text{eV}$ ,  $\Delta H_f(\text{rock-salt GeTe}) = -0.364\text{eV}$ ,  $\Delta H_f(\text{rhombohedral Sb}_2\text{Te}_3) = -1.222\text{eV}$ .

As Te is deficient, the atomic chemical potentials are estimated to be -0.376, -0.391, -0.352 eV for  $\mu_{Te}$  in GST225, GST124 and GST147, respectively, which correspondingly produce the formation energies of  $\text{Sb}_{\text{Te}1}$  to be 0.126, 0.258 and 0.324 eV, respectively. In this case, the  $\text{Sb}_{\text{Te}1}$  concentrations are calculated to be  $1.66 \times 10^{21} \text{ cm}^{-3}$ ,  $4.40 \times 10^{20} \text{ cm}^{-3}$  and  $2.38 \times 10^{20} \text{ cm}^{-3}$  with a synthesis temperature 1000K in GST225, GST124 and GST147, respectively. Consequently,  $\text{Sb}_{\text{Te}1}$  is the predominated defect at a Te deficient environment, which results in the *p*-type conductivity. Moreover, as seen in Fig. 1 (d) which shows the  $\text{Sb}_{\text{Te}}$  concentration as a function of temperature with Te deficiency, the  $\text{Sb}_{\text{Te}}$  concentration in GST225 is the highest among the three investigated compounds. This is in contrast to the above assumption of the  $\text{Sb}_{\text{Te}}$  concentration increasing as the increase of  $\text{Sb}_2\text{Te}_3$  building block in GST.

At the condition of Sb deficiency, the estimated atomic chemical potential  $\mu_{Sb} = -0.941$ , -0.782, -0.616 eV for GST225, GST124 and GST147, respectively. As a result, the formation energies for  $\text{Te}_{\text{Sb}}$  are -0.003, 0.011 and 0.317 eV in GST225, GST124 and GST147, respectively, which will respectively produce  $\text{Te}_{\text{Sb}}$  concentrations of  $7.43 \times 10^{21} \text{ cm}^{-3}$ ,  $7.74 \times 10^{21} \text{ cm}^{-3}$  and  $2.58 \times 10^{20} \text{ cm}^{-3}$  with synthesized temperature of 1000K. However, this does not imply that electrons will be the majority charge carrier as the  $V_{\text{Sb}}$  concentration will also increase drastically with Sb deficiency. For example in GST225,

with Sb deficiency the formation energy of one  $V_{Sb}$  will be -0.143 that indicates the spontaneous formation of antimony vacancies. In this case, the  $V_{Sb}$  concentration is  $1.35 \times 10^{22} \text{ cm}^{-3}$  at 1000 K, which is much higher than that of  $Te_{Sb}$ . Together with the large  $V_{Ge}$  concentration, the majority charge carrier in GST225 is still holes and the conductivity remains a *p*-type character. While in GST124 and GST147, the  $V_{Sb}$  concentrations are  $1.35 \times 10^{18}$  and  $1.01 \times 10^{18} \text{ cm}^{-3}$ , respectively, which are the same order as that of  $V_{Ge}$  but are 3 and 2 orders lower than the  $Te_{Sb}$  concentration, respectively. Therefore, it is likely  $Te_{Sb}$  is the majority defect and *n*-type conductivity can be achieved in GST124 and GST147. It is clear that GST225 always has *p*-type conductivity, while it is possible to make both *p* and *n* type conductivity in GST124 and GST147. This is good for thermoelectric applications as both *p* and *n* type conduction can be achieved in one type of material. The present results show a picture of multi-carriers of both holes and electrons in GST, where the majority charge carrier can be tuned by varying synthesis chemical environment except GST225 which always exhibit *p*-type behavior.

Fig. 2 shows the total density of states for GST225 of ideal and defect states. It is seen that the Fermi level of ideal GST225 locates between the conduction band and valence band, while for the defective compounds, the Fermi level locates within a small tail of valence band states for  $V_{Ge}$  and  $Sb_{Te}$  containing-system which results from  $V_{Ge}$  and  $Sb_{Te}$ . For  $Te_{Sb}$  antisite defective GST225, the Fermi level locates within a small tail of conduction band states which comes from  $Te_{Sb}$ . Furthermore, even though with present DFT calculations, one can not obtain accurate band gap, a trend obtained from Fig. 2 is that the band gap narrows with the presence of point defects.

Analyses on the electron localization function (ELF) reveals that the introduction of defects results in slight changes just around the defects. Fig. 3 (a) and (b) shows the ELF projected on the (110) plane for  $V_{Ge}$  and  $Sb_{Te}$  containing GST225, respectively. As seen in Fig. 3 (a), non-bonded electrons at Te1 and Te2 facing the Ge vacancy position are clearly seen and the Te2-Sb covalent bond as well as weak Te3-Te4 bond turns to stronger. With the presence of  $Sb_{Te}$  as shown in Fig. 3 (b), the Sb2-Sb<sub>Te1</sub> covalent bond and stronger Sb<sub>Te1</sub>-Te2 bond turns to stronger. Nevertheless, the introduction of vacancies and antisite defects only results in slight changes in the chemical bonding around the defects. Moreover, slight change in  $a$  lattice parameters but obvious decrease in  $c$  lattice parameters are found by the presence of vacancies and antisite defects, which will be present in an extensive paper in the future.

In summary, the majority defects in GST are  $V_{Ge}$  and  $Sb_{Te}$  which results in the  $p$ -type conductivity. The defects formation energies of various types are the lowest in GST225, and hence the highest defect concentrations. Furthermore, GST225 are always  $p$ -type semiconductors at the condition of various atomic chemical potentials, while it is possible to make both  $p$  and  $n$  type conductivity in GST124 and GST147 by tuning the synthesis environments. Finally, the introduction of defects only changes the chemical bonding character just around the defect in the building chains.

This work is supported by National Natural Science Foundation of China (60976005), the Outstanding Young Scientists Foundation of Fujian Province of China (2010J06018) and the program for New Century Excellent Talents in University (NCET-08-0474).

- <sup>1</sup> Ü. Özgür *et al.*, J. Appl. Phys. **98**, 041301 (2005).
- <sup>2</sup> P. P. Konstantinov *et al.*, Inorganic Mater. **37**, 662 (2001).
- <sup>3</sup> J. M. Yanez-Limon *et al.*, Phys. Rev. B **52**, 16321 (1995).
- <sup>4</sup> H.-K. Lyeo *et al.*, Appl. Phys. Lett. **89**, 151904 (2006).
- <sup>5</sup> S. Raoux, W. Welnic and D. Lelmini, Chem. Rev. **110**, 240 (2010).
- <sup>6</sup> B.-S. Lee and S. G. Bishop, in *Phase Change Materials: Science and Applications*, edited by S. Raoux, M. Wuttig, Springer Science+Business Media, LLC 2009.
- <sup>7</sup> A. V. Kolobov, J. Non-Crystalline solids 198-200, 728 (1996).
- <sup>8</sup> A. H. Edwards *et al.*, J. Phys. Condens. Matter. **17**, L329 (2005).
- <sup>9</sup> J. Horak, L. Koudelka, J. Klikorka, Reactivity of Solids **5**, 351 (1988).
- <sup>10</sup> G. Kresse and J. Furthmüller, Phys. Rev. B **54**, 11169 (1996);
- <sup>11</sup> P. E. Blöchl, Phys. Rev. B **50**, 17953 (1994).
- <sup>12</sup> J. P. Perdew, K. Burke, M. Ernzerhof, Phys Rev Lett. **77**, 3865 (1996).
- <sup>13</sup> L. E. Shelimova *et al.*, Inorganic Mater. **37**, 342 (2001).
- <sup>14</sup> Z. M. Sun, J. Zhou, R. Ahuja, Phys. Rev. Lett. **96**, 055507 (2006).
- <sup>15</sup> Z. M. Sun *et al.*, Solid State Commu. **143**, 240 (2007).
- <sup>16</sup> S. B. Zhang *et al.*, Phys. Rev. B **57**, 9642 (1998).
- <sup>17</sup> S. B. Zhang, J. E. Northrup, Phys. Rev. Lett. **67**, 2339 (1991).
- <sup>18</sup> H.-K. Lyeo *et al.*, Appl. Phys. Lett. **89**, 151904 (2006).
- <sup>19</sup> Y. Jung *et al.*, J. Am. Chem. Soc. **128**, 14026 (2006).

## Figure captions

FIG. 1 (Color online) The concentration of various types of defects as a function of synthesis temperature for (a)  $\text{Ge}_2\text{Sb}_2\text{Te}_5$ , (b)  $\text{GeSb}_2\text{Te}_4$ , (c)  $\text{GeSb}_4\text{Te}_7$  and (d) the Te deficient condition

FIG. 2 The calculated total density of states for (a) stoichiometry  $\text{Ge}_2\text{Sb}_2\text{Te}_5$ , defective  $\text{Ge}_2\text{Sb}_2\text{Te}_5$  containing (b)  $\text{Te}_{\text{Sb}}$ , (c)  $\text{V}_{\text{Ge}}$  and (d)  $\text{Sb}_{\text{Te1}}$ .

FIG. 3 (color online) The ELF projected on the (110) planes for defective  $\text{Ge}_2\text{Sb}_2\text{Te}_5$  containing (a)  $\text{V}_{\text{Ge}}$  and (b)  $\text{Sb}_{\text{Te1}}$ , where the scale is from 0 (blue) to 1 (red) and the interval is 0.14.

## Table captions

Table I. Formation energies of isolated neutral point defects (in eV) in layered GST compounds.

Table I.

	Antisite			$V_{\text{Ge}}$	Vacancy		
	$\text{Sb}_{\text{Te1}}$	$\text{Sb}_{\text{Te2}}$	$\text{Te}_{\text{Sb}}$		$V_{\text{Sb}}$	$V_{\text{Te1}}$	$V_{\text{Te2}}$
GST225	0.502	0.785	0.938	0.350	0.798	1.705	1.503
GST124	0.649	0.922	0.793	0.577	1.539	—	—
GST147	0.676	0.898	0.936	0.565	1.411	—	—

Fig. 1 of Sun et al submitted to PRB with a manuscript No. LW12097BR

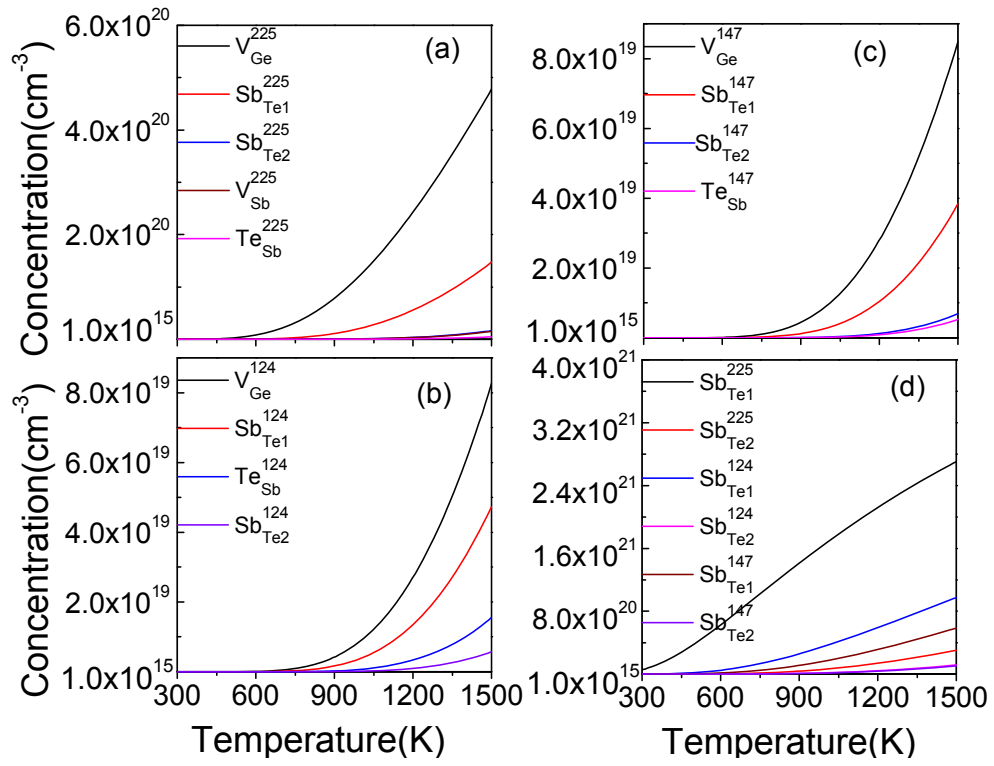


Fig. 2 of Sun et al submitted to PRB with a manuscript No. LW12097BR

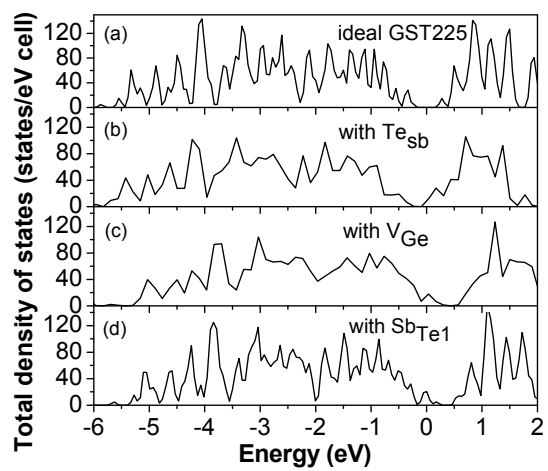


Fig. 3 of Sun et al submitted to PRB with a manuscript No. LW12097BR

